Ions colliding with clusters of fullerenes—Decay pathways and covalent bond formations

F. Seitz,[1] H. Zettergren,[1,a)] P. Rousseau,[2,3] Y. Wang,[4,5] T. Chen,[1] M. Gatchell,[1] J. D. Alexander,[1] M. H. Stockett,[1] J. Rangama,[2] J. Y. Chesnel,[2,3] M. Capron,[2,3] J. C. Poully,[2,3] A. Domaracka,[2] A. Méry,[2,3] S. Maclot,[2,3] V. Vizcaino,[2] H. T. Schmidt,[1] L. Adoui,[2,3] M. Alcamí,[4] A. G. G. M. Tielens,[6] F. Martín,[4,5] B. A. Huber,[2] and H. Cederquist[1]

[1]*Department of Physics, Stockholm University, S-106 91 Stockholm, Sweden*
[2]*CIMAP, UMR 6252, CEA/CNRS/ENSICAEN/Université de Caen Basse-Normandie, bd Henri Becquerel, BP 5133, F-14070 Caen cedex 05, France*
[3]*Université de Caen Basse-Normandie, Esplanade de la Paix, F-14032 Caen, France*
[4]*Departamento de Química, Módulo 13, Universidad Autónoma de Madrid, 28049 Madrid, Spain*
[5]*Instituto Madrileño de Estudios Avanzados en Nanociencia (IMDEA-Nano), Cantoblanco, 28049 Madrid, Spain*
[6]*Leiden University, Leiden Observatory, NL-2300 RA Leiden, Netherlands*

(Received 23 April 2013; accepted 18 June 2013; published online 17 July 2013)

We report experimental results for the ionization and fragmentation of weakly bound van der Waals clusters of n C_{60} molecules following collisions with Ar^{2+}, He^{2+}, and Xe^{20+} at laboratory kinetic energies of 13 keV, 22.5 keV, and 300 keV, respectively. Intact singly charged C_{60} monomers are the dominant reaction products in all three cases and this is accounted for by means of Monte Carlo calculations of energy transfer processes and a simple Arrhenius-type $[C_{60}]_n^+ \rightarrow C_{60}^+ + (n-1)C_{60}$ evaporation model. Excitation energies in the range of only ~0.7 eV per C_{60} molecule in a $[C_{60}]_{13}^+$ cluster are sufficient for complete evaporation and such low energies correspond to ion trajectories far outside the clusters. Still we observe singly and even doubly charged intact cluster ions which stem from even more distant collisions. For penetrating collisions the clusters become multiply charged and some of the individual molecules may be promptly fragmented in direct knock-out processes leading to efficient formations of new covalent systems. For Ar^{2+} and He^{2+} collisions, we observe very efficient C_{119}^+ and C_{118}^+ formation and molecular dynamics simulations suggest that they are covalent dumb-bell systems due to bonding between C_{59}^+ or C_{58}^+ and C_{60} during cluster fragmentation. In the Ar^{2+} case, it is possible to form even smaller C_{120-2m}^+ molecules ($m = 2$–7), while no molecular fusion reactions are observed for the present Xe^{20+} collisions. © *2013 AIP Publishing LLC*. [http://dx.doi.org/10.1063/1.4812790]

I. INTRODUCTION

Why is it that certain fullerenes, such as C_{60} and C_{70}, are much more abundantly produced than those with other (even) numbers of carbon atoms? This is a main and still not fully resolved question since the discovery[1] of this intriguing class of all-carbon molecules. One appealing recent suggestion is the so called hot shrinking giant fullerene route in which hot giant fullerene-like molecular structures with more than 60 or 70 atoms and often with adducts are first spontaneously assembled in a carbon plasma and then decay by first losing those adducts and later sequences of C_2-molecules. In this scenario, the slightly higher binding energy per atom of C_{60} and C_{70} compared to their neighbours explains their high abundances.[2] An even more recent, and equally appealing suggestion, is a bottom-up formation mechanism in which fullerene growth is explained as sequential inclusions of single C-atoms or C_2-molecules in smaller fullerenes and here the critical aspect is the exceptionally low reactivity of C_{60} or C_{70}[3] compared to their neighbours. In a recent experiment in which *large* van der Waals clusters of C_{60} fullerenes, $[C_{60}]_n$ with $n \sim 100$, were exposed to high energy Xe^{20+}-ions, the formation of giant hot fullerenes was observed.[4] This was explained as being due to the shattering of fullerenes along the ion tracks in small fragments which had time to reassemble to giant fullerenes due to outer shells of intact C_{60} molecules.[4] In the same experiment, the measured high formation rate of C_{70} was rationalized as sequential absorptions of C-atoms and small carbon molecules in outer undamaged C_{60} molecules,[4] similar to what was proposed in Ref. 3. Recently, we reported on covalent bond formation reactions induced in interactions between somewhat smaller clusters of C_{60} and keV He^{2+} ions.[5] We then found that these reactions are very different from those induced when such clusters are heated by photo-absorption,[6] as we observed efficient formations of covalent C_{119}^+ and C_{118}^+ *dumb-bell* structures. Such processes are initiated by prompt carbon knock-outs in nuclear stopping processes.[5] Here, we further investigate these intriguing issues by increasing the nuclear stopping energy by

a)Author to whom correspondence should be addressed. Electronic mail: henning@fysik.su.se

using the heavier Ar^{2+} projectiles. For comparison, we will also show results for $He^{2+}/Xe^{20+} + [C_{60}]_n$ collisions. In the present study, the sizes of the clusters have mostly been limited to considerably smaller values of n, $n \sim 5$–20, than in Ref. 4.

Following the recent spectroscopic identifications of infrared emission from C_{60} and C_{70} in space[7,8] there have been suggestions for how these molecules may be formed in low density environments. Possibly, this may occur through UV-processing of Polycyclic Aromatic Hydrocarbons (PAHs).[9] Interactions with ions could lead to different PAH-destruction processes than photo-absorption and thus processing by H^+ and He^{2+} in plasma shocks could well be important here.[10]

In the following, we will first give a brief presentation of the experimental technique by which several charged fragments may be recorded in coincidence. The experimental results are analyzed and discussed with the aid of: (i), a classical over-the-barrier description of ionization processes; (ii) Monte Carlo calculations of energy-transfer distributions for ion interactions with clusters and monomers of C_{60} (electronic and nuclear stopping processes); (iii) a simple Arrhenius-type cluster evaporation model; and (iv) Molecular Dynamics (MD) simulations of chemical reactions induced by prompt ion-induced atom knock-out processes in individual C_{60} molecules in the cluster.[5]

II. EXPERIMENTAL TECHNIQUE AND PROCEDURES

The experiments were performed at the ARIBE facility at GANIL in Caen, France. A detailed description of this facility is given in Ref. 11. Briefly, keV ion beams are produced in an Electron Cyclotron Resonance (ECR) ion source and then pulsed by switching voltages on deflection plates at a repetition rate of a few kHz. The microsecond long beam pulses interact with cold (∼80 K) clusters of fullerenes produced in a liquid nitrogen cooled cluster aggregation source. The distribution of cluster sizes most likely follows a log-normal distribution.[12] The positively charged collision products are analyzed with the aid of a linear time-of-flight mass spectrometer.[13] The ions hit a gold coated steel plate at the end of the spectrometer from which the emitted secondary electrons are guided to a microchannel plate (MCP) detector by a weak magnetic field. This detector system has a high detection efficiency, and thus allows for coincidence measurements of several fragment ions from single collision events.

III. REACTION SCENARIOS

Here we will rely on the classical over-the-barrier concept which is well known to give good estimates of the maximum distances at which electrons may transfer from an initially neutral target to a projectile ion. Charge transfer models based on this concept have been developed for point-like atomic targets,[14] fullerenes (spherical targets),[15–17] surfaces,[18] and very recently for planar molecules such as PAHs (circular discs).[19] For high projectile charge states, the critical distances for electron transfer to the ion are large. In the fullerite bulk limit and for large clusters of fullerenes, the work function of 4.7 eV[20] indicates that electrons may be removed at distances up to 37 a_0[18] from the cluster surfaces by Xe^{20+} projectiles. For Xe^{20+} colliding with, e.g., $[C_{60}]_{13}$ these assumptions give a total ionization cross section of 3.4×10^{-13} cm^2. For Ar^{2+} or He^{2+} the first critical distance lies 12.3 a_0 outside the cluster surface yielding a cross section of 1.2×10^{-13} cm^2 for $[C_{60}]_{13}$. Here, the total ionization cross sections include single- and multiple-ionization and related cluster fragmentation processes. Second critical distances, at which second electrons may move from the target to the projectile, lie 35.9 a_0 and 9.2 a_0 outside cluster surfaces for Xe^{20+}- or Ar^{2+}/He^{2+} projectiles, respectively. At such large distances, very little energy should be transferred to the clusters in stopping processes, and a projectile ion P in charge state q ionizes a target cluster softly

$$P^{q+} + [C_{60}]_n \rightarrow P^{(q-s)+} + [C_{60}]_n^{r+} + (r-s)e^-, \qquad (1)$$

such that $[C_{60}]_n^{r+}$ may remain intact on the time scale of the experiment (tens to hundreds of microseconds). The number of electrons removed from the cluster is r and s is the number of electrons captured by the projectile $s \leq r$. For somewhat closer collisions but where impact parameters still are larger than the cluster radius, one or several electrons are removed and the cluster is heated such that it always decays. Normally this gives reactions of the type

$$P^{q+} + [C_{60}]_n \rightarrow P^{(q-s)+} + (n-r)C_{60} + rC_{60}^+ + (r-s)e^-. \qquad (2)$$

For low values of q, the number of electrons removed from the target is small, and since the C_{60}-C_{60} binding energies are very small compared to the internal C_{60} binding energies, the clusters mainly decay by sequential emission of neutral C_{60} molecules leaving relatively cold C_{60}^+ ions as end products. For large values of q in reactions described by Eq. (2), many electrons are removed leading to Coulomb explosions which heat the C_{60}^+ fragments such that they may decay further through C_2-emission. For cluster-penetrating collisions, reactions according to Eq. (2) may occur especially for light projectile ions in low charge states. In addition, the individual C_{60} molecules may be fragmented promptly in some collisions, and then new covalent systems larger than C_{60} may form.

IV. EXPERIMENTAL RESULTS FOR SMALL CLUSTER SIZES

In Fig. 1 we show the ionization and fragmentation spectra for $[C_{60}]_n$ clusters in 13 keV $Ar^{2+} + [C_{60}]_n$, 22.5 keV $He^{2+} + [C_{60}]_n$, and 300 keV $Xe^{20+} + [C_{60}]_n$ collisions. The results discussed in this section are mainly for small target cluster sizes ($n \sim 5$–20).

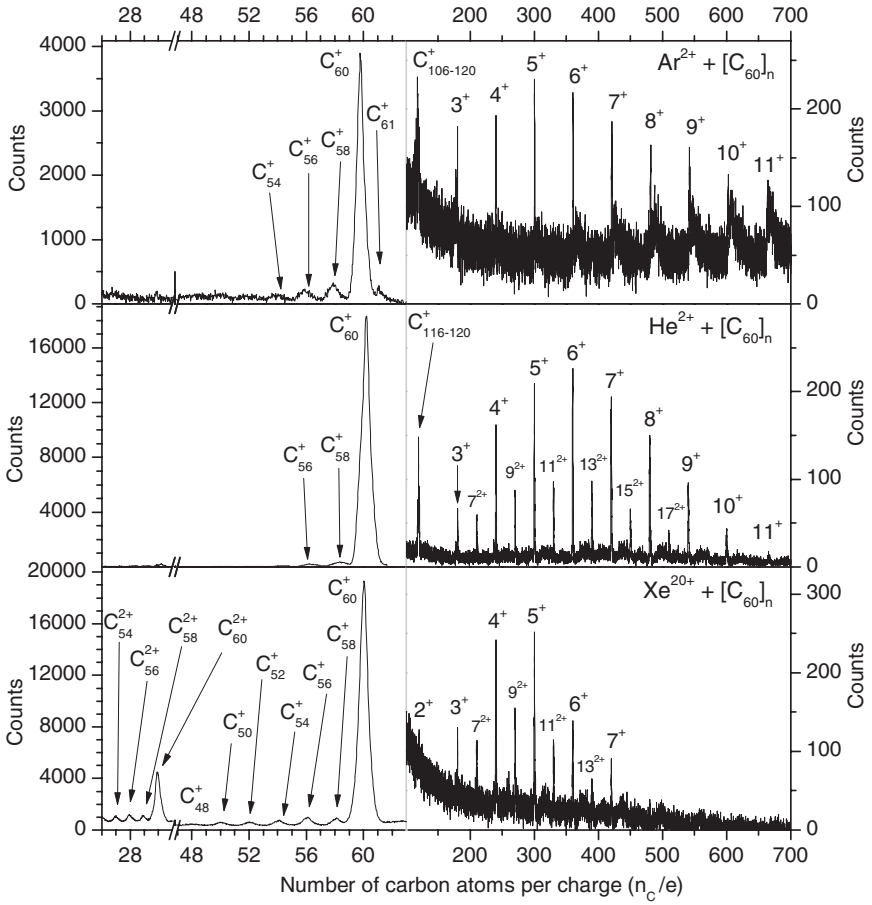

FIG. 1. Mass-to-charge spectra for collisions between ions at keV energies and small clusters of C_{60} molecules. From top to bottom: 13 keV Ar^{2+}+$[C_{60}]_n$, 22.5 keV He^{2+}+$[C_{60}]_n$, and 300 keV Xe^{20+}+$[C_{60}]_n$ collisions. The left panels show details of the fragment spectra in the regions around the singly and doubly charged monomers. The right panels show details for larger masses per atomic unit of charge ($n_C/e = 100$ to 700). Note the differences between left and right hand intensity scales.

A. Total ionization and fragmentation spectra: Ar^{2+} impact

The upper panels of Fig. 1 show that the C_{60}^+ peak is dominant with much less intense peaks at C_{58}^+, C_{56}^+, C_{54}^+, etc. for 13 keV Ar^{2+} + $[C_{60}]_n$ collisions. The latter fragments are most likely due to sequences of C_2-emissions from the few hotter of the C_{60}^+ ions emitted in the cluster fragmentation processes. The main picture here is thus that these weakly bound clusters most often are multiply ionized and distribute their charge and internal excitation energy on the molecular building blocks before fragmentation which mainly yields neutral and singly charged C_{60} molecules.

Relatively few of the C_{60}^+ products are sufficiently hot for further fragmentation on the experimental time scale of microseconds. Surprisingly, a C_{61}^+ peak is also clearly visible in the upper left panel of Fig. 1. We believe that this is caused by fragmentation of one or several C_{60} molecules in the cluster and absorption of C atoms from such fragmentation processes by intact C_{60} molecules during cluster fragmentation. In a recent study,[3] the mass spectra following laser ablation of a fullerene-graphite mixture showed clear evidence of molecular growth processes in which fullerenes larger than C_{60} and with even numbers of carbon atoms were produced. As we will demonstrate below, a C_{62}^+ peak will also appear on the side of C_{61}^+ when we increase the cluster sizes. Our observation of a C_{61}^+ peak is thus consistent with the ideas of efficient single C-inclusion in the C_{60} cage structure as presented in Ref. 3. However, C_{61} ions were not observed directly in that experiment.[3]

The narrow components of the peaks in the upper right panel of Fig. 1 are due to clusters of C_{60} molecules which have been singly ionized in collisions with Ar^{2+} and which remain intact during extraction and acceleration in the time-of-flight spectrometer (cf. Eq. (1)). These narrow peaks are labelled n^+ and correspond to singly charged, intact, $[C_{60}]_n^+$ clusters with n ranging from $n = 3$ to 11. For the larger n in this range the peaks have, in addition, strong tails which mainly are due to decays of larger clusters ($n > 11$) in the extraction region of the spectrometer.

B. Total ionization and fragmentation spectra: He^{2+} impact

In the He^{2+} + $[C_{60}]_n$ case, the C_{60}^+ peak again dominates strongly but is broader than for Ar^{2+} projectiles (cf. Fig. 1). Although simple classical over-the-barrier estimates yield identical critical distances for ionization by Ar^{2+} and He^{2+}, there are on closer inspection some differences having

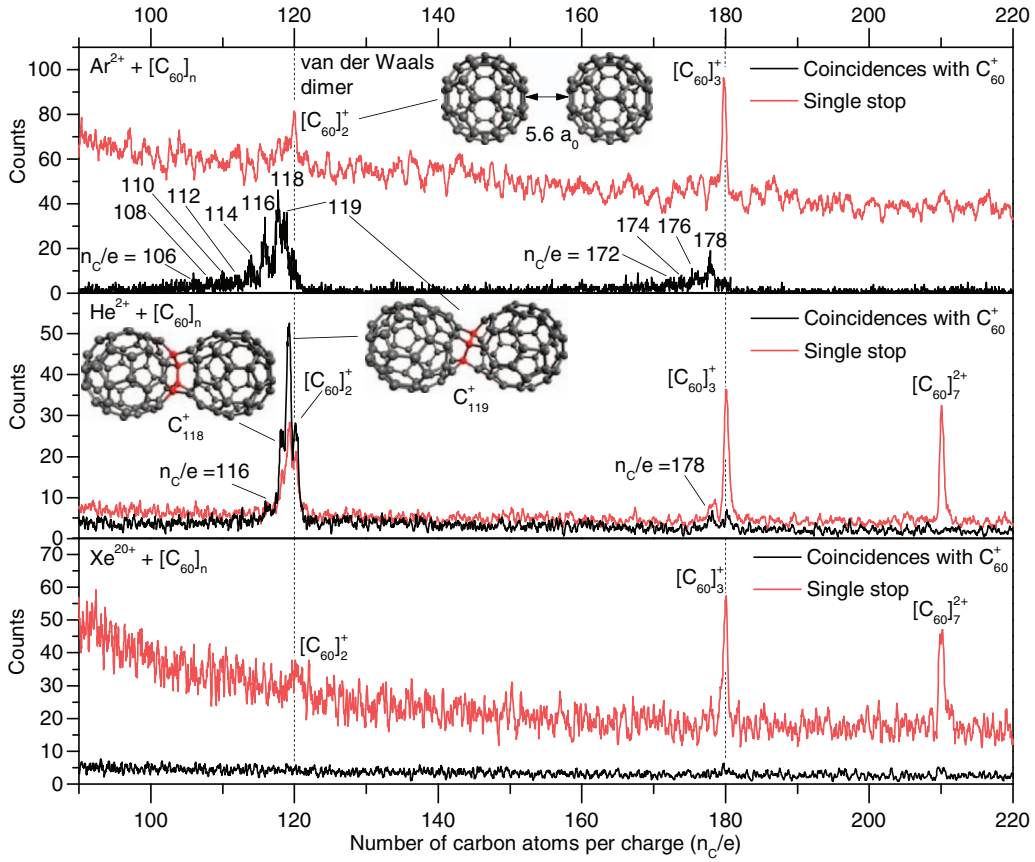

FIG. 2. Parts of the mass-to-charge spectra due to 13 keV Ar^{2+}+$[C_{60}]_n$, 22.5 keV He^{2+}+$[C_{60}]_n$, and 300 keV Xe^{20+}+$[C_{60}]_n$ collisions for small clusters of C_{60}. The red curves show the singles event spectra – only one ion detected per collision event. The black curves show events recorded in coincidence with one or several C_{60}^+ ions. For C_{118}^+ and C_{119}^+ (middle panel) structures obtained from DFT calculations are shown (cf. text).

to do with the much deeper potential well of the He^{2+} nucleus in comparison with the Ar^{2+} core. The second ionization energies of Ar and He are about 27 eV and 54 eV, respectively. Thus He^{2+} projectiles will in practice be much more efficient in removing several electrons from the cluster targets leading to higher cluster charge states, larger intracluster Coulomb repulsions, and larger C_{60}^+ kinetic energies in the fragmentation processes. For He^{2+} we observe narrow peaks due to doubly ionized intact clusters in the range between $[C_{60}]_7^{2+}$ and $[C_{60}]_{17}^{2+}$. The C_{58}^+, C_{56}^+, etc. fragment peaks are much less intense with He^{2+} than with Ar^{2+} and this is because emitted C_{60}^+ are colder on the average for the He^{2+} case.

C. Total ionization and fragmentation spectra: Xe^{20+} impact

For the Xe^{20+} + $[C_{60}]_n$ collisions, the distribution of cluster sizes in the target is centered on slightly smaller n than in the Ar^{2+} and the He^{2+} cases. This can be seen from the intensity distributions of the narrow $[C_{60}]_n^+$, and $[C_{60}]_n^{2+}$, peaks in the three right panels of Fig. 1. The mass-to-charge spectrum for the Xe^{20+} collisions exhibits a dominant and wide C_{60}^+ peak, a longer series of C_{60-2m}^+ fragments than for He^{2+} and Ar^{2+}, a rather strong C_{60}^{2+} peak with a C_{60-2m}^{2+} series, and narrow $[C_{60}]_n^+$ and $[C_{60}]_n^{2+}$ peaks. With Xe^{20+} and limited target cluster sizes it is possible to remove more than one electron per C_{60} molecule already at large distances and this is the reason for the rather strong C_{60}^{2+} peak in the lower left panel of Fig. 1. It has been established earlier that charge redistributes very rapidly within ionized clusters of C_{60} molecules[21,22] and that the Coulomb explosion heats the individual molecules strongly.[23]

D. Formation of dumb-bell shaped molecules

In Fig. 2, we show single-stop and coincidence data for the region between $n_C/e = 90$ and $n_C/e = 220$. In the single-stop case, only one ion from each collision event has been detected, while the spectra labeled "coincidences with C_{60}^+" are events which have been detected in coincidence with one or several C_{60}^+ ions. In the single stop spectrum for Ar^{2+} + $[C_{60}]_n$, we observe narrow peaks corresponding to $[C_{60}]_2^+$ and $[C_{60}]_3^+$ but no peak due to $[C_{60}]_7^{2+}$. The latter peak is clearly present in the single-stop data for He^{2+} and Xe^{20+} and the fact that it is missing for Ar^{2+} is due to strong cluster heating in double ionization processes as discussed above. In the Ar^{2+} and He^{2+} coincidence data, we observe peaks at $n_C/e = 119$, 118, 116, and 178. In the Ar^{2+} case, there are also peaks from $n_C/e = 114$ and down to $n_C/e = 106$ and from $n_C/e = 176$ and down. With the aid of molecular dynamics simulations and molecular structure calculations,[5] we have recently shown that C_{119}^+ and C_{118}^+ may be efficiently

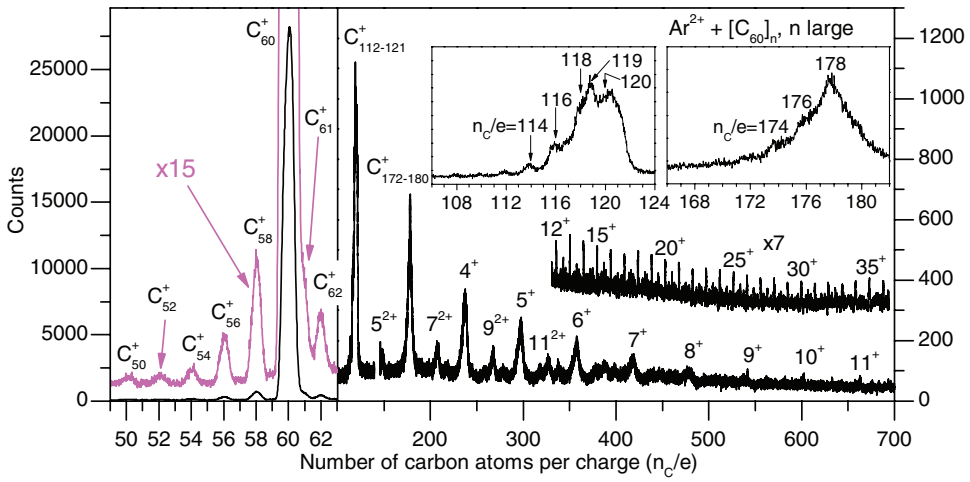

FIG. 3. Mass-to-charge spectrum for collisions between 12 keV Ar^{2+} ions and large clusters of C_{60} molecules. The left panel shows details of the singly charged monomer region in black and a zoomed-in version (×15) of the same spectral region in magenta. The right panel shows the high-mass region. The ×7 inset shows the spectrum in the interval 700–2000 n_C/e. The upper insets show details of the dimer (120 n_C/e) and trimer (180 n_C/e) regions.

formed in their dumb-bell forms indicated in the middle panel of Fig. 2. The key here is that fullerenes in the clusters are partly fragmented in prompt few-atom knock-out processes. The so formed C_{59}^+ and C_{58}^+ ions are very reactive and they easily form dumb-bell systems in barrier-less reactions with C_{60} before the clusters decay, which typically takes a few picoseconds.[5] The C_{60}^+ ions, on the other hand, which are produced in much larger numbers than C_{59}^+ and C_{58}^+, have high barriers against $C_{60}^+ + C_{60}$ fusion reactions. The C_{120}^+ dumb-bell is very difficult to form – it requires kinetic energies in the range of 60 eV.[5] We attribute the much richer distribution of molecular fusion products with Ar^{2+} to the higher probabilities for multiple knock-outs. Thus, highly reactive smaller fragments are more efficiently formed in the Ar^{2+} case. The peaks just below $n_C/e = 180$ are due to covalently bound systems with three fullerene-like cages and from the molecular dynamics simulations[5] we see that these systems are preferentially formed at lower kinetic energies in the sub- to few eV range. For the present $Xe^{20+} + [C_{60}]_n$ collisions where n is comparatively low, there are no indications of molecular fusion processes as can be seen in the lowest panel of Fig. 2. However, strong molecular fusion processes have been observed previously for Xe^{20+} projectiles but then with much larger clusters in the target.[4]

V. COLLISIONS WITH LARGER CLUSTERS

In Fig. 3 we show the total mass-to-charge spectrum for $Ar^{2+} + [C_{60}]_n$ collisions where we have used much larger $[C_{60}]_n$ clusters in the target than for the corresponding spectrum in Fig. 1. Having larger clusters in the target leads to dramatic changes in the spectrum (compare Fig. 3 and the upper panels in Fig. 1). With larger clusters, the C_{60-2m}^+ fragments become weaker in relation to the C_{60}^+ peak and this is readily explained as larger clusters give a more effective cooling of the individual molecules as locally induced excitation energy and charge are distributed on the whole cluster before fragmentation.[22,24] The C_{61}^+ peak is present for small and large clusters but in the case of large n (Fig. 3) it is also accompanied by a significant C_{62}^+ peak. The C_{61}^+ and C_{62}^+ peaks may be due to the absorption of one and two C-atoms in a C_{60} molecule, and/or to absorption of one C_2-molecule for C_{62}^+. Again, this observation relates to the discussion by Dunk *et al.* in Ref. 3 based on their experiments with laser ablation of C_{60}-graphite mixtures. There, the details of general bottom-up fullerene formation mechanisms were discussed and the inclusion of single C-atoms and single C_2-molecules in C_{60} was considered to be a crucial step.[3]

No narrow peaks corresponding to singly charged $[C_{60}]_n$ clusters are visible below $n = 10$ for $Ar^{2+} + [C_{60}]_n$ collisions when n is large. This is due to the fact that larger clusters, which have decayed through long sequences of emissions of neutral or singly charged C_{60} molecules (cf. below), leave behind singly ionized small clusters with rather large kinetic energies and this gives symmetrically broadened peaks. At the same time, some of the larger clusters above roughly $n = 10$ may remain intact as the excitation energy may distribute on a larger number of molecular building blocks in large clusters. This can be seen from the narrow peaks in the region above $n = 10$ (cf. the large-mass region with the ×7 zoom-in factor in one of the insets in Fig. 3). We observe the same $C_{59}^+ + C_{60} \rightarrow C_{119}^+$, $C_{58}^+ + C_{60} \rightarrow C_{118}^+$ etc. molecular fusion processes for $Ar^{2+} + [C_{60}]_n$ with large (Fig. 3) as with small clusters (Fig. 1) but with larger intensities in Fig. 3.

VI. ENERGY DEPOSITION AND CLUSTER FRAGMENTATION

A. Monte Carlo calculation of stopping energies

In the upper panel of Fig. 4, we show results for Monte Carlo calculations of electronic stopping distributions for Ar^{2+} colliding with C_{60} monomers, and clusters of C_{60} molecules $[C_{60}]_n$ for $n = 2$, 7, 13, 19, and 55. In all cases there are peaks on the low energy side and these peaks are mainly due to non-penetrating peripheral collisions which transfers at least a certain amount of energy to the target (a few eV). The electronic stopping distributions have maxima in the

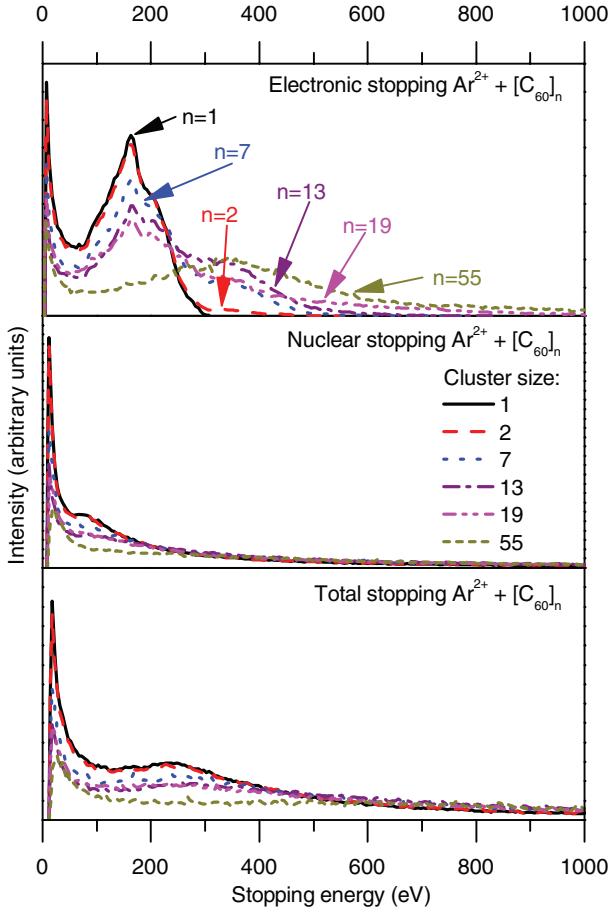

FIG. 4. Results from Monte Carlo calculations of electronic (top), nuclear (middle), and total stopping energies for 12 keV Ar^{2+} colliding with $[C_{60}]_n$ clusters with $n = 1$ (the monomer), $n = 2$, 7, 13, 19, and 55 (cf. text).

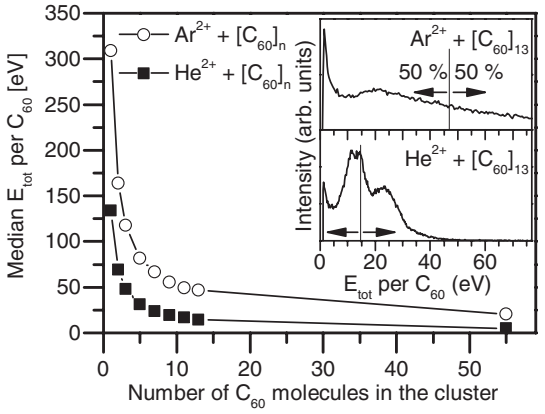

FIG. 5. Median total stopping energies (E_{tot}) per C_{60} molecule in the cluster for collisions between 12 keV Ar^{2+} or 22.5 keV He^{2+} ions and C_{60} clusters of different sizes. The insets show the distributions for clusters with 13 molecules. The median values for $[C_{60}]_{13}$ are indicated by vertical lines in the insets. Lines between data points are to guide the eye.

150–200 eV region corresponding to ions passing through one C_{60} molecule and there are maxima at roughly twice this energy for ions passing through two molecules. The probability for the latter increases with cluster size. For the largest cluster considered in the present calculations, $[C_{60}]_{55}$, the probability to go through three or more fullerenes is significant and gives a high energy tail. In the middle panel of Fig. 4, we show the energy loss distributions from nuclear stopping processes while the total energy loss distributions (sum of electronic and nuclear stopping for each ion trajectory) are shown in the lower panel. We use the Monte Carlo approach to launch large numbers of ion trajectories at randomly oriented C_{60} molecules or clusters of such molecules. The energy losses due to electronic stopping processes are calculated along the ion trajectory using electron densities from density functional theory calculations (level B3LYP/STO-3G) and friction coefficients deduced from Ref. 25. The nuclear energy loss is obtained through the well-established method described for example by Larsen *et al.*[26]

In Fig. 5 we show median values for the total energy loss per C_{60} molecule in the cluster as a function cluster size. The deposited energy is shared between the individual molecules such that they become cold enough to stay intact and to be detected as C_{60}^+ on the present experimental time scale for large enough clusters. For this the internal C_{60}^+ energy has to be in the range of about 50 eV or below as has been measured directly by Martin *et al.*[27] and this is indeed the case for the median energy per molecule for clusters larger than about $n = 10$ for 13 keV $Ar^{2+} + [C_{60}]_n$ collisions. For He^{2+} collisions at 22.5 keV much less energy is transferred for a given cluster size and this readily explains why the emitted C_{60}^+ ions are colder and more often stay intact for He^{2+}- than for Ar^{2+}-collisions (cf. the upper and middle left panels in Fig. 1).

The individual C_{60} molecules in the clusters have high internal binding energies and thus large dissociation energies. The energy required for C_2-emission is about 10 eV[28] and the ions may stay intact on the experimental time scale. The situation is different for clusters due to the very weak C_{60}-C_{60} bonds and these will often dissociate completely even in rather distant single- or multiple-ionization processes.

B. Modelling cluster fragmentation

Clusters of fullerenes are weakly bound with dissociation energies (E_d) of about 0.3 eV,[22] and they form evaporative ensembles at rather low temperatures (T_{evap}). In a simple Arrhenius type decay picture,[29] $T_{evap} = E_d/(k_B G)$, where k_B is the Boltzmann constant and G is the so-called Gspann factor. Thus, $T_{evap} = 150$ K for $G = 23.5$, i.e., for a G-value which has been frequently used for atomic and molecular clusters decaying on the 10 μs-timescale.[29] In Fig. 6, we show the minimum energy per molecule which is required for complete evaporation of $[C_{60}]_n^+$ clusters $[C_{60}]_n^+ \rightarrow [C_{60}]_{n-1}^+ + C_{60} \rightarrow [C_{60}]_{n-2}^+ + C_{60} + C_{60} \rightarrow \ldots \rightarrow C_{60}^+ + (n-1)C_{60}$ with initial sizes between $n = 2$ and $n = 55$. Here we follow Schmidt *et al.*[29] and treat the intermolecular vibrations classically and use the internal C_{60} vibrations from Ref. 30 to calculate the cluster temperatures after each evaporation step. As the major part of the internal energy is stored in the individual molecules the temperature decreases slowly as a function of the number of evaporation steps, which means that long evaporation sequences are needed to cool down moderately heated clusters below T_{evap}. As an example, an internal energy slightly larger than 1.2 eV per molecule (400 K) is

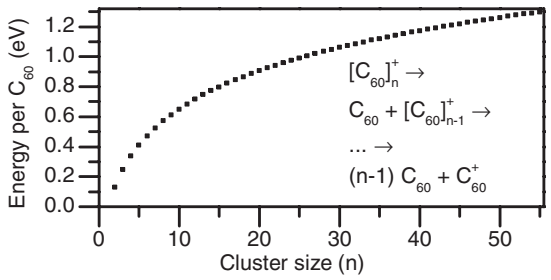

FIG. 6. The minimum energy per molecule which is required for complete evaporation of $[C_{60}]_n^+$ clusters according to a simple statistical model where the clusters are assumed to form an evaporative ensemble at $T_{evap} = 150$ K (cf. text).

sufficient for complete evaporation of a $[C_{60}]_{55}^+$ cluster, which is significantly lower than the typical energy transferred in penetrating collisions (cf. Figs. 4 and 5). This explains why the singly charged monomer peak is dominant in all mass spectra due to collisions with ions in low charge states as, e.g., Ar^{2+} and He^{2+}. From these considerations it also seems reasonable to attribute the corresponding intact cluster distributions in Figs. 1 and 3 to the most distant ionizing collisions where very low amounts of energy are transferred to the clusters.

VII. SUMMARY AND CONCLUSIONS

In summary, we have compared the processing of weakly bound clusters of fullerenes for three different keV-projectiles (Ar^{2+}, He^{2+}, and Xe^{20+}). The most distant electron transfer collisions leave the ionized clusters sufficiently cold to survive the experimental μs-timescale, while peripheral and penetrating collisions induce fragmentation with the singly charged monomer being the dominant end product in all three cases. For low charge state projectiles (He^{2+}/Ar^{2+}) the fragmentation processes are mainly thermally activated, leading to long evaporation sequences down to the monomer even for moderately heated clusters. For high charge state projectiles (Xe^{20+}), the singly charged monomer fragments stem from charge driven fragmentation processes. The latter leads to strong internal heating of the individual molecules. We find that weakly bound clusters of fullerenes most likely will separate in its molecular building blocks following collisions with keV ions in both high and low charge states.

The lighter projectiles (Ar^{2+} and He^{2+}) may knock out single carbon atoms such that highly reactive large fragments with odd number of carbons (e.g., C_{59}^+) and adjacent pentagons (e.g., C_{58}^+) are produced. These efficiently form covalent dumb-bell systems (e.g., C_{119}^+ and C_{118}^+) in reactions with neighbouring C_{60} molecules before the clusters decay. The energy transfer increases for heavier projectiles leading to a stronger propensity for multiple carbon loss, and thus a more rich distribution of covalent bound systems for Ar^{2+} than for He^{2+} projectiles. In the Xe^{20+} case, the fullerene cages are completely disintegrated in penetrating collisions, which readily explains why covalent bond modifications are not observed for collisions with clusters of moderate size. The observation of C_{61}^+ and C_{62}^+ ions produced in collisions between Ar^{2+} and clusters of fullerenes is most likely due to the absorptions of single C-atoms and or C_2 molecules in individual C_{60} molecules. This lends support to bottom-up fullerene assembly mechanisms in which inclusions of single C atoms is assumed to be a key ingredient.[3] Single atom knock-out by ion/atom impact may be important processes for understanding astrochemical reactions. These processes, which hitherto have been overlooked, may be efficient routes to the formation of larger molecules in clusters, dust grains, or in other aggregates of matter in space.

ACKNOWLEDGMENTS

This work was supported by the Swedish Research Council (Contract Nos. 621-2008-3773, 621-2009-3468, and 621-2011-4047). The authors thank Fabien Noury and Stephane Guillous for supplying the ion beam. We acknowledge the COST action CM1204 "XUV/X-ray light and fast ions for ultrafast chemistry (XLIC)" and computer time from CCC-UAM and BSC Mare Nostrum. Work partially supported by Project Nos. FIS2010-15127, CTQ2010-17006, CSD2007-00010 (MICINN), S2009/MAT1726 (CAM), and the CNRS PICS-05356. Studies of interstellar chemistry at Leiden Observatory are supported through advanced-ERC grant (Grant No. 246976) from the European Research Council, through a grant by the Dutch Science Agency, NWO, as part of the Dutch Astrochemistry Network, and through the Spinoza premie from the Dutch Science Agency, NWO.

[1] H. W. Kroto, J. R. Heath, S. C. Obrien, R. F. Curl, and R. E. Smalley, Nature (London) **318**, 162 (1985).
[2] S. Irle, G. Zheng, Z. Wang, and K. Morokuma, J. Chem. Phys. B **110**, 14531 (2006).
[3] P. W. Dunk, N. K. Kaiser, C. L. Hendrickson, J. P. Quinn, C. P. Ewels, Y. Nakanishi, Y. Sasaki, H. Shinohara, A. G. Marshall, and H. W. Kroto, Nat. Commun. **3**, 855 (2012).
[4] H. Zettergren, H. A. B. Johansson, H. T. Schmidt, J. Jensen, P. Hvelplund, S. Tomita, Y. Wang, F. Martin, M. Alcami, B. Manil, L. Maunoury, B. A. Huber, and H. Cederquist, J. Chem. Phys. **133**, 104301 (2010).
[5] H. Zettergren, P. Rousseau, Y. Wang, F. Seitz, T. Chen, M. Gatchell, J. D. Alexander, M. H. Stockett, J. Rangama, J. Y. Chesnel, M. Capron, J. C. Poully, A. Domaracka, A. Méry, S. Maclot, H. T. Schmidt, L. Adoui, M. Alcamí, A. G. G. M. Tielens, F. Martín, B. A. Huber, and H. Cederquist, Phys. Rev. Lett. **110**, 185501 (2013).
[6] M. Hedén, K. Hansen, and E. E. B. Campbell, Phys. Rev. A **71**, 055201 (2005).
[7] J. Cami, J. Bernard-Salas, E. Peeters, and S. E. Malek, Science **329**, 1180 (2010).
[8] D. A. García-Hernández, A. Manchado, P. García-Lario, L. Stanghellini, E. Villaver, R. A. Shaw, R. Szczerba, and J. V. Perea-Calderón, Astrophys. J. Lett. **724**, L39 (2010).
[9] O. Berné and A. G. G. M. Tielens, Proc. Natl. Acad. Sci. U.S.A. **109**, 401 (2012).
[10] E. R. Micelotta, A. P. Jones, J. Cami, E. Peeters, J. Bernard-Salas, and G. Fanchini, Astrophys. J. **761**, 35 (2012).
[11] T. Bergen, X. Biquard, A. Brenac, F. Chandezon, B. A. Huber, D. Jalabert, H. Lebius, M. Maurel, E. Monnand, J. Opitz, A. Pesnelle, B. Pras, C. Ristori, and J. C. Rocco, Rev. Sci. Instrum. **70**, 3244 (1999).
[12] J. Maul, T. Berg, E. Marosits, G. Schönhense, and G. Huber, Phys. Rev. B. **74**, 161406(R) (2006).
[13] F. Chandezon, B. A. Huber, and C. Ristori, Rev. Sci. Instrum. **65**, 3344 (1994).
[14] A. Bárány, G. Astner, H. Cederquist, H. Danared, S. Huldt, P. Hvelplund, A. Johnson, H. Knudsen, L. Liljeby, and H.-G. Rensfelt, Nucl. Instrum. Methods Phys. Res. B **9**, 397 (1985).
[15] A. Bárány and C. J. Setterlind, Nucl. Instrum. Methods Phys. Res. B **98**, 184 (1995).

[16]H. Cederquist, A. Fardi, K. Haghighat, A. Langereis, H. T. Schmidt, S. H. Schwartz, J. C. Levin, I. A. Sellin, H. Lebius, B. Huber, M. O. Larsson, and P. Hvelplund, Phys. Rev. A **61**, 022712 (2000).
[17]H. Zettergren, B. O. Forsberg, and H. Cederquist, Phys. Chem. Chem. Phys. **14**, 16360 (2012).
[18]J. Burgdörfer, P. Lerner, and F. W. Meyer, Phys. Rev. A **44**, 5674 (1991).
[19]B. O. Forsberg, J. D. Alexander, T. Chen, A. T. Pettersson, M. Gatchell, H. Cederquist, and H. Zettergren, J. Chem. Phys. **138**, 054306 (2013).
[20]G. Gensterblum, K. Hevesi, B.-Y. Han, L.-M. Yu, J.-J. Pireaux, P. A. Thiry, R. Caudano, A.-A. Lucas, D. Bernaerts, S. Amelinckx, G. Van Tendeloo, G. Bendele, T. Buslaps, R. L. Johnson, M. Foss, R. Feidenhans'l, and G. Le Lay, Phys. Rev. B **50**, 11981 (1994).
[21]H. Zettergren, H. T. Schmidt, P. Reinhed, H. Cederquist, J. Jensen, P. Hvelplund, S. Tomita, B. Manil, J. Rangama, and B. A. Huber, J. Chem. Phys. **126**, 224303 (2007).
[22]H. Zettergren, Y. Wang, A. M. Lamsabhi, M. Alcamí, and F. Martín, J. Chem. Phys. **130**, 224302 (2009).
[23]A. I. S. Holm, H. Zettergren, H. A. B. Johansson, F. Seitz, S. Rosén, H. T. Schmidt, A. Ławicki, J. Rangama, P. Rousseau, M. Capron, R. Maisonny, L. Adoui, A. Méry, B. Manil, B. A. Huber, and H. Cederquist, Phys. Rev. Lett. **105**, 213401 (2010).
[24]B. Manil, L. Maunoury, B. A. Huber, J. Jensen, H. T. Schmidt, H. Zettergren, H. Cederquist, S. Tomita, and P. Hvelplund, Phys. Rev. Lett. **91**, 215504 (2003).
[25]M. J. Puska and R. M. Nieminen, Phys. Rev. B **27**, 6121 (1983).
[26]M. Larsen, P. Hvelplund, M. Larsson, and H. Shen, Eur. Phys. J. D **5**, 283 (1999).
[27]L. Chen, S. Martin, J. Bernard, and R. Brédy, Phys. Rev. Lett. **98**, 193401 (2007).
[28]S. Tomita, J. U. Andersen, C. Gottrup, P. Hvelplund, and U. V. Pedersen, Phys. Rev. Lett. **87**, 073401 (2001).
[29]M. Schmidt, A. Masson, and C. Bréchignac, Int. J. Mass Spectrom. **252**, 173 (2006).
[30]J. Menéndez, and J. B. Page, in *Light Scattering in Solids VIII*, Topics in Applied Physics Vol. 76, edited by M. Cardona and G. Güntherodt (Springer, Berlin, 2000), pp. 27–95.